JOURNAL OF COMPUTATIONAL PHYSICS 37, 183–204 (1980)

An Iterative Metric Method for Solving the Inverse Tokamak Equilibrium Problem

J. DELUCIA, S. C. JARDIN, AND A. M. M. TODD

Plasma Physics Laboratory, Princeton University, Princeton, New Jersey 08540

Received July 2, 1979; revised October 5, 1979

A method is presented for solving the toroidal magnetohydrodynamic equilibrium equation in a coordinate system based on the magnetic field lines. Both fixed boundary (conducting shell) and free boundary (external coil) boundary conditions are considered. A comparison with a special analytic solution is made. The method is useful for obtaining equilibria to use in tokamak stability and transport calculations.

I. INTRODUCTION

The calculation of axisymmetric solutions to the magnetohydrodynamic equilibrium equation $\nabla p = \mathbf{J} \times \mathbf{B}$ plays a central role in tokamak stability and transport studies, as well as in the design of future toroidal devices. Methods for solving the toroidal equilibrium equation in the Grad–Shafranov form,

$$(2\pi)^{-2} x^2 \nabla \cdot (x^{-2} \nabla \chi) + 4\pi x^2 p' + x_0^2 g g' = 0, \tag{1}$$

have been known for some time [1–4]. Here $\chi(x, z)$ is the poloidal magnetic flux function, $p(\chi)$ is the fluid pressure, $x_0 g(\chi) \equiv x^2 \mathbf{B} \cdot \nabla \phi$ is the toroidal field function, (x, ϕ, z) form a cylindrical coordinate system, and $'$ denotes $\partial/\partial\chi$.

For many tokamak stability studies, it is not $\chi(x, z)$ that is needed but rather $\chi(\psi)$ and the inverse functions $x(\theta, \psi)$ and $z(\theta, \psi)$, where (ψ, θ) are generalized magnetic flux coordinates with properties to be described in Section II. To obtain these inverse functions numerically, one typically solves the Grad–Shafranov equation for $\chi(x, z)$ on a rectangular grid by standard methods and then employs a mapping procedure [5] to contour levels of constant ψ and θ. Thus, the (x, z) coordinates of the intersection of the contours $\theta_i \equiv i\delta\theta$ and $\psi_j \equiv j\delta\psi$ form a discrete set of points $(x_{i,j}; z_{i,j}) \equiv [x(\theta_i, \psi_j); z(\theta_i, \psi_j)]$ which collectively define a finite difference approximation to the exact mapping $[x(\theta, \psi); z(\theta, \psi)]$.

The discrete mapping obtained in this manner is often adequate but in general satisfies the flux coordinate form of the finite differenced equilibrium equation only to within some error introduced by truncation error in the original (x, z) solution and in

0021-9991/80/110183-22$02.00/0

the contouring. The fact that this error is limited by the truncation error inherent in the finite difference equations rather than by an iteration tolerance (which can be made arbitrarily small) can render this method unacceptable for producing equilibrium for some sensitive stability studies. Also, when solving for equilibrium with large values of $\beta \equiv 8\pi p/B^2$, the magnetic axis shift is comparable to the minor radius, $\Delta \sim a$, and large local gradients of flux and current can arise. A difference method based on equal increments in real space is not optimal for resolving these spaially local steep gradients.

We discuss in this paper the iterative metric method, a finite difference method for solving for the discrete coordinate functions $(x_{i,j}; z_{i,j})$ such that the flux coordinate form of the finite differenced equilibrium equation based on these points is satisfied to an arbitrarily small tolerance. In addition, the numerical grid on which finite differences are evaluated is tied to the equilibrium solution itself in such a way that grid points automatically accumulate in regions of steep gradients.

In Section II the problem is mathematically defined by introducing the (ψ, θ) coordinate system and expressing the equilibrium equation in these coordinates. In Section III the basic solution method is presented for the case where the shape of the plasma/vacuum interface does not change (fixed boundary). This forms the core of the more involved procedure, described in Section IV, for solving the free boundary problem in which currents in external coils define the boundary conditions. The location of the plasma/vacuum interface is then determined as part of the solution. Both of these methods are illustrated in Section V, where some numerical solutions are presented. Verification is accomplished by computing an equilibrium for which an exact solution exists.

II. Flux Coordinates and the Equilibrium Equation

If the magnetic field lines in an axisymmetric tokamak plasma form nested toroidal surfaces, the coordinates (ψ, θ, ϕ) can be defined (see Fig. 1) such that ψ is constant on these surfaces (i.e., $\mathbf{B} \cdot \nabla\psi = 0$), θ is a periodic poloidal coordinate, ϕ is the toroidal symmetry angle, and the Jacobian is of the form

$$\mathscr{J} \equiv (\nabla\psi \times \nabla\theta \cdot \nabla\phi)^{-1} = \mu(x/x_0)^m \psi^n.$$

Here $0 \leqslant \theta < 2\pi$, $0 \leqslant \phi < 2\pi$, $0 \leqslant \psi \leqslant 1$, μ and x_0 are constants included for normalization, and m and n are arbitrary integers. The vectors $\nabla\psi$ and $\nabla\theta$ are both orthogonal to $\nabla\phi$ but are not necessarily orthogonal to each other. By appropriately choosing m and n, several axisymmetric nonorthogonal magnetic flux coordinate systems discussed previously can be obtained [5–7].

Gradients and divergences can be evaluated in these coordinates by noting that for any axisymmetric scalar a and vector $\mathbf{A}$,

$$\nabla a = a_\psi \nabla\psi + a_\theta \nabla\theta, \tag{2a}$$

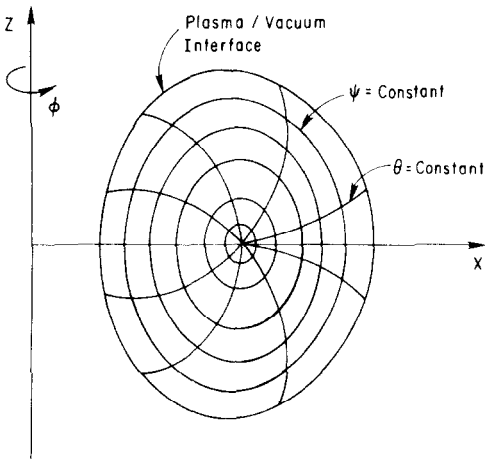

FIG. 1. Nonorthogonal flux coordinate system, (ψ, θ, ϕ), used in solving the inverse tokamak equilibrium problem. ψ is a flux coordinate, θ a poloidal angle coordinate, and ϕ the toroidal symmetry angle.

and

$$\begin{aligned}\mathcal{J}\nabla\cdot\mathbf{A} = &[(\nabla\theta\times\nabla\phi\cdot\mathbf{A})x^2\mathcal{J}h^{\psi\psi} + (\nabla\phi\times\nabla\psi\cdot\mathbf{A})x^2\mathcal{J}h^{\psi\theta}]_\psi \\ &+[(\nabla\theta\times\nabla\phi\cdot\mathbf{A})x^2\mathcal{J}h^{\psi\theta} + (\nabla\phi\times\nabla\psi\cdot\mathbf{A})x^2\mathcal{J}h^{\theta\theta}]_\theta.\end{aligned} \tag{2b}$$

Here, the Jacobian $\mathcal{J}$ and the metric elements $h^{\alpha\beta} \equiv x^{-2}\mathcal{J}\nabla\alpha\cdot\nabla\beta$ can be expressed as derivatives of the cylindrical spatial coordinates (x, z):

$$\mathcal{J} = x(x_\psi z_\theta - x_\theta z_\psi), \tag{2c}$$

$$h^{\psi\psi} = (x_\theta^2 + z_\theta^2)/\mathcal{J}, \tag{2d}$$

$$h^{\theta\theta} = (x_\psi^2 + z_\psi^2)/\mathcal{J}, \tag{2e}$$

$$h^{\psi\theta} = -(x_\theta x_\psi + z_\theta z_\psi)/\mathcal{J}. \tag{2f}$$

Subscripts are used to denote differentiation with respect to ψ and θ.

By using Eqs. (2) to evaluate the first term in Eq. (1) and noting that by definition, $\chi = \chi(\psi)$ (i.e., $\chi_\theta = 0$), the inverse equilibrium equation takes the form

$$\begin{aligned}\Delta^*\chi(\psi) \equiv x^2\nabla\cdot x^{-2}\nabla\chi(\psi) &= x^2\mathcal{J}^{-1}[(\chi_\psi h^{\psi\psi})_\psi + (\chi_\psi h^{\psi\theta})_\theta] \\ &= -(2\pi)^2(4\pi x^2 p' + x_0^2 gg'),\end{aligned} \tag{3a}$$

and the Jacobian constraint requires that (x, z) satisfy

$$x(x_\psi z_\theta - x_\theta z_\psi) = \mu(x/x_0)^m\psi^n. \tag{3b}$$

Given the functions $p(\chi)$ and $g(\chi)$ and the appropriate boundary conditions, Eq. (3)

can be regarded as an equation for $\chi(\psi)$ and for the two-dimensional coordinate functions $x(\theta, \psi)$ and $z(\theta, \psi)$.

In practice, it is convenient to prescribe the value of the total plasma current when solving Eq. (3). In this case, the functional forms of the fluid pressure $p(\chi)$, and the toroidal field function $g(\chi)$, are taken to be of the form

$$p(\chi) = p_b + (p_0 - p_b)\chi_s^{\alpha}, \tag{4a}$$

and

$$g(\chi) = 1 - \gamma\chi_s^{\beta}, \tag{4b}$$

where

$$\chi_s \equiv [\chi(1) - \chi(\psi)]/[\chi(1) - \chi(0)]. \tag{4c}$$

Here γ is determined by the requirment that the total plasma current remain fixed; i.e.,

$$I_T = -2\pi \int_0^1 d\psi \int_0^{2\pi} d\theta \mathscr{J}[p' + (4\pi)^{-1}(x_0/x)^2 gg'], \tag{5}$$

p_0 and p_b are the specified values of pressure at the magnetic axis and plasma boundary, and α and β are input parameters.

Once $\chi(\psi)$, $x(\theta, \psi)$, and $z(\theta, \psi)$ are known, the magnetic field and current can be obtained from the defining relations

$$\mathbf{B} = (2\pi)^{-1}\chi_{\psi}(\psi)\,\nabla\phi \times \nabla\psi + x_0 g(\psi)\,\nabla\phi, \tag{6}$$

and

$$\mathbf{J} = \mathscr{J}[(\mathbf{J} \cdot \nabla\theta)\,\nabla\phi \times \nabla\psi + (\mathbf{J} \cdot \nabla\phi)\,\nabla\psi \times \nabla\theta]. \tag{7}$$

The components of $\mathbf{J}$ come from Ampere's law:

$$\mathbf{J} \cdot \nabla\theta = -\mathscr{J}^{-1} x_0 g_{\psi}/4\pi, \tag{8a}$$

$$\mathbf{J} \cdot \nabla\phi = \nabla \cdot (\chi_{\psi} x^{-2}\,\nabla\psi)/8\pi^2. \tag{8b}$$

The safety factor $q(\psi)$ is obtained by performing a surface integral on a constant ψ surface,

$$q(\psi) \equiv \int_0^{2\pi} \frac{d\theta}{2\pi} \frac{\mathbf{B} \cdot \nabla\phi}{\mathbf{B} \cdot \nabla\theta} = x_0 g\langle x^{-2}\rangle V_{\psi}/(2\pi\chi_{\psi}), \tag{9a}$$

where the brackets denote flux surface average,

$$\langle a\rangle \equiv \int_0^{2\pi} d\theta \mathscr{J} a \Big/ \int_0^{2\pi} d\theta \mathscr{J},$$

and $V_\psi \equiv \partial(\int_0^\psi d\mathbf{x})/\partial\psi = 2\pi \int_0^{2\pi} \mathscr{J}\, d\theta$. Equation (9a) can be used to eliminate the toroidal field function g from the equilibrium equation (3a) in favor of the safety factor q. As discussed in Ref. [2], the form of the equilibrium equation so obtained, with $p(\chi)$ and $q(\chi)$ as the two free functions, is often convenient to use in stability studies. From Eq. (9a), we have

$$x_0^2 gg' = (2\pi)^2 \left(\frac{\chi_\psi q}{\langle x^{-2}\rangle V_\psi}\right)_\psi \frac{q}{\langle x^{-2}\rangle V_\psi}, \tag{9b}$$

and from surface averaging Eq. (3a), and using Eq. (9b),

$$\left(\chi_\psi \left\langle \frac{h^{\psi\psi}}{\mathscr{J}} \right\rangle V_\psi\right)_\psi = -(2\pi)^2 \left[4\pi V_\psi p' + (2\pi)^2 q \left(\frac{\chi_\psi q}{\langle x^{-2}\rangle V_\psi}\right)_\psi\right]. \tag{10}$$

Now, $\chi_{\psi\psi}$ can be eliminated from Eq. (9b) using Eq. (10), and the result can be combined with Eqs. (3) to express the equilibrium equation as

$$[(2\pi)^{-2}\Delta^* - A(\partial/\partial\psi)]\chi = -4\pi B p'. \tag{11a}$$

Here

$$A = \frac{(2\pi)^2 q^3}{D\langle x^{-2}\rangle^3 V_\psi^3} \left(\left\langle \frac{h^{\psi\psi}}{\mathscr{J}} \right\rangle V_\psi^2 \frac{\langle x^{-2}\rangle}{q}\right)_\psi, \tag{11b}$$

$$B = \left[\left(x^2 - \frac{1}{\langle x^{-2}\rangle}\right)\left(\frac{(2\pi)^4 q^2}{\langle x^{-2}\rangle V_\psi}\right) + x^2 V_\psi \left\langle \frac{h^{\psi\psi}}{\mathscr{J}} \right\rangle\right] \Big/ D, \tag{11c}$$

$$D = \left(V_\psi \left\langle \frac{h^{\psi\psi}}{\mathscr{J}} \right\rangle + \frac{(2\pi)^4 q^2}{\langle x^{-2}\rangle V_\psi}\right). \tag{11d}$$

Equation (11a) is the form of the equilibrium equation solved numerically when the functions $p(\chi)$ and $q(\chi)$ are given. Using

$$p(\chi) = p_0\{\Lambda - 1\}^\alpha, \tag{11e}$$

$$q(\chi) = q_0\{2/\Lambda\}^\beta, \tag{11f}$$

where $\Lambda = \{1 + 3[\chi(1) - \chi(\psi)]/[\chi(1) - \chi(0)]\}^{1/2}$, we have produced the high β equilibrium reported in Ref. [8] and discussed in more detail in Section V. When specifying $q(\chi)$ in this manner, a further constraint is imposed, that the total poloidal flux, $\Delta\chi \equiv \chi(1) - \chi(0)$, remain fixed.

III. Fixed Boundary Solution Method

The iterative metric method of solving the equilibrium equation inside of a plasma/vacuum interface whose shape is held fixed consists of the following steps:

A. Guess an initial coordinate transformation corresponding to iteration level $k = 0$,

$$(x^0_{i,j},\ z^0_{i,j}); \qquad i = 1, M; \qquad j = 1, N.$$

This initial transformation must have a Jacobian finite everywhere except possibly at $j = 1$, the magnetic axis. The points corresponding to $j = N$ define the plasma boundary.

B. Solve the generalized coordinate equilibrium equation for the poloidal flux at the new iteration level, $k + 1$, using the coordinate transformation at the old iteration level, k; i.e., obtain $\tilde{\chi}^{(k+1)}$ by solving the finite difference form of the equilibrium equation (3a),

$$(2\pi)^{-2}\Delta^{*(k)}\tilde{\chi}^{(k+1)} = -\{4\pi x^{2(k)}p'[\tilde{\chi}^{(k+1)}] + \tfrac{1}{2}x_0^2(g^2)'[\tilde{\chi}^{(k+1)}]\}, \tag{12a}$$

where

$$\Delta^{*(k)} \equiv (x^2\mathscr{J}^{-1})^{(k)}\{(\partial/\partial\psi)[h^{\psi\psi(k)}(\partial/\partial\psi) + h^{\psi\theta(k)}(\partial/\partial\theta)] + (\partial/\partial\theta)[h^{\psi\theta(k)}(\partial/\partial\psi) + h^{\theta\theta(k)}(\partial/\partial\theta)]\}, \tag{12b}$$

or of the equilibrium equation (11a),

$$[(2\pi)^{-2}\Delta^{*(k)} - A^{(k)}(\partial/\partial\psi)]\tilde{\chi}^{(k+1)} = -4\pi B^{(k)}p'[\tilde{\chi}^{(k+1)}]. \tag{12c}$$

As a boundary condition on Eqs. (12a) and (12c) we take $\tilde{\chi}(\theta, 1) = 0$.

C. Interpolate using the poloidal flux at the new iteration level, $\tilde{\chi}^{(k+1)}_{i,j}$, to define the coordinate functions at the new iteration level, $x^{(k+1)}_{i,j}$ and $z^{(k+1)}_{i,j}$, such that the finite difference forms of the requirement that the poloidal flux be constant along constant ψ surfaces and that the Jacobian have the form of Eq. (3b) are satisfied; i.e.,

(i) $\tilde{\chi}^{(k+1)}_{\theta} = 0$, and

(ii) $[x(x_{\psi}z_{\theta} - x_{\theta}z_{\psi})]^{(k+1)} = \mu[x^{(k+1)}/x_0]^m\psi^n$.

D. Iterate Steps B and C until the poloidal flux at the end of Step B is independent of θ to some tolerance.

Next, Steps A through C will be described in more detail.

Step A

An initial coordinate transformation is constructed as follows: Define the shape of the plasma boundary by giving the Cartesian coordinates of N boundary points, $\{x^0_{i,N};\ z^0_{i,N}: i = 1, M\}$. The interior points are then defined by

$$x^0_{i,j} = (\psi_j)^{(n+1)/2}(x^0_{i,N} - R) + R,$$
$$z^0_{i,j} = (\psi_j)^{(n+1)/2}z^0_{i,N},$$

where $i = 1,..., M$; $j = 1,..., N$. The point corresponding to $x = R$ and $z = 0$ must lie in

the interior of the curve defined by the M boundary points. For example for a D-shaped plasma boundary, we choose the boundary points to be

$$x_{i,N} = R + a\cos(\theta_i + \delta \sin\theta_i),$$
$$z_{i,N} = \varepsilon a \sin\theta_i,$$

where R, a, ε, and δ are constants.

Step B

Either Eq. (12a) or Eq. (12c) is solved numerically for the poloidal flux at the new iteration level, $k+1$. The finite difference form of Eq. (12b) is

$$\begin{aligned}
&\Delta^{*(k)}\tilde{\chi}^{(k+1)} \\
&\quad \equiv x^2\mathscr{J}^{-1(k)}\big[-(H^{\psi\psi}_{i,j+1/2} + H^{\psi\psi}_{i,j-1/2} + H^{\theta\theta}_{i+1/2,j} + H^{\theta\theta}_{i+1/2,j})\tilde{\chi}^{(k+1)}_{i,j} \\
&\qquad + (H^{\psi\theta}_{i-1/2,j} + H^{\psi\theta}_{i,j-1/2})\tilde{\chi}^{(k+1)}_{i-1,j-1} + (H^{\psi\psi}_{i,j-1/2} - H^{\psi\theta}_{i+1/2,j} + H^{\psi\theta}_{i-1/2,j})\tilde{\chi}^{(k+1)}_{i,j-1} \\
&\qquad - (H^{\psi\theta}_{i+1/2,j} + H^{\psi\theta}_{i,j-1/2})\tilde{\chi}^{(k+1)}_{i+1,j-1} - (H^{\psi\theta}_{i,j+1/2} - H^{\psi\theta}_{i,j-1/2} - H^{\psi\theta}_{i-1/2,j})\tilde{\chi}^{(k+1)}_{i-1,j} \\
&\qquad - (H^{\psi\theta}_{i,j+1/2} + H^{\psi\theta}_{i-1/2,j})\tilde{\chi}^{(k+1)}_{i-1,j+1} + (H^{\psi\theta}_{i,j+1/2} - H^{\psi\theta}_{i,j-1/2} + H^{\theta\theta}_{i+1/2,j})\tilde{\chi}^{(k+1)}_{i+1,j} \\
&\qquad + (H^{\psi\theta}_{i+1/2,j} + H^{\psi\theta}_{i,j+1/2})\tilde{\chi}^{(k+1)}_{i+1,j+1} + (H^{\psi\psi}_{i,j+1/2} + H^{\psi\theta}_{i+1/2,j} - H^{\psi\theta}_{i-1/2,j})\tilde{\chi}^{(k+1)}_{i,j+1}\big], \qquad (13)
\end{aligned}$$

where

$$H^{\psi\psi} = [h^{\psi\psi}/(\delta\psi)^2]^{(k)}, \qquad (14a)$$
$$H^{\psi\theta} = [h^{\psi\theta}/(4\delta\psi\delta\theta)]^{(k)}, \qquad (14b)$$
$$H^{\theta\theta} = [h^{\theta\theta}/(\delta\theta)^2]^{(k)}. \qquad (14c)$$

The metric terms $h^{\psi\psi}$, $h^{\psi\theta}$, $h^{\theta\theta}$, $\mathscr{J}$ and the surface averages V_ψ, $\langle x^{-2}\rangle$, $\langle h^{\psi\psi}/\mathscr{J}\rangle$ are evaluated from the finite difference forms of Eqs. (2c) through (2f) using centered difference operators on $[x^{(k)}_{ij}, z^{(k)}_{ij}]$. Either Eq. (12a) or Eq. (12c), together with the boundary condition $\tilde{\chi}^{(k+1)}_{i,N} = 0$, is solved for $\tilde{\chi}^{(k+1)}$ by the successive over-relaxation method. Before each over-relaxation sweep begins either γ is readjusted to keep the total plasma current a constant (p and g prescribed) or $\tilde{\chi}$ is scaled everywhere to keep $\tilde{\chi}(1) - \tilde{\chi}(0)$ constant (p and q prescribed). Thus, for the p and g method, we define

$$p'(\tilde{\chi}) \equiv -\frac{\alpha(p_0 - p_b)}{\Delta\tilde{\chi}}\left(\frac{\tilde{\chi}(1) - \tilde{\chi}}{\Delta\tilde{\chi}}\right)^{\alpha-1},$$

$$g_1(\tilde{\chi}) \equiv \frac{\beta}{\Delta\tilde{\chi}}\left(\frac{\tilde{\chi}(1) - \tilde{\chi}}{\Delta\tilde{\chi}}\right)^{\beta-1},$$

$$g_2(\tilde{\chi}) \equiv \frac{\beta}{\Delta\tilde{\chi}}\left(\frac{\tilde{\chi}(1) - \tilde{\chi}}{\Delta\tilde{\chi}}\right)^{2\beta-1},$$

$$\Delta\tilde{\chi} \equiv \tilde{\chi}(1) - \tilde{\chi}(0).$$

Then γ is adjusted to satisfy the quadratic equation

$$I_T = -2\pi \sum_{i=1}^{M} \sum_{j=1}^{N} \delta\psi\delta\theta \mathscr{J}_{i,j} \left[p'(\tilde{\chi}_{i,j}) + \gamma(4\pi)^{-1} \left(\frac{x_0}{x}\right)^2_{i,j} g_1(\tilde{\chi}_{i,j}) - \gamma^2(4\pi)^{-1} \left(\frac{x_0}{x}\right)^2_{i,j} g_2(\tilde{\chi}_{i,j}) \right].$$

We note here that if $\tilde{\chi}$ is a solution to the fixed boundary problem, then $\tilde{\chi}$ plus any constant is also a solution. We choose the constant in this section so that $\tilde{\chi}$ vanishes on the boundary. In the next section, it is shown that this constant is determined in the free boundary problem by the requirement that χ match onto a vacuum solution which vanishes at infinity.

The point $\psi = 0$ is a singularity in the (ψ, θ, ϕ) coordinate system and thus requires special treatment. To obtain the value of $\tilde{\chi}$ at that point we assume that $\tilde{\chi}$ is analytic there and has a Taylor series expansion of the form

$$\tilde{\chi} = a^{00} + a^{10}x + a^{01}z + a^{20}x^2 + a^{11}xz + a^{22}z^2 + \cdots, \tag{15a}$$

where the a^{ij} are constants. It can be shown from Eq. (3b) that x and z have a Fourier series expansion about the origin of the form

$$x = R + b^x_{10}\psi^{(n+1)/2}(1 + b^x_{11}\psi^{n+1} + \cdots)\cos\theta + b^x_{20}\psi^{(n+1)}(1 + b^x_{21}\psi^{n+1} + \cdots)\cos 2\theta + \cdots, \tag{15b}$$

$$z = b^z_{10}\psi^{(n+1)/2}(1 + b^z_{11}\psi^{n+1} + \cdots)\sin\theta + b^z_{20}\psi^{n+1}(1 + b^z_{21}\psi^{n+1} + \cdots)\sin 2\theta + \cdots, \tag{15c}$$

where the b^α_{ij} are constants. Substituting Eqs. (15b) and (15c) into Eq. (15a) and averaging over the angle θ gives an expansion for the surface averaged poloidal flux,

$$\overline{\tilde{\chi}(\psi)} = \tilde{\chi}^0 + b\psi^{(n+1)} + c\psi^{2(n+1)} + \cdots. \tag{16}$$

Here the surface average operator has been defined as

$$\overline{\tilde{\chi}(\psi)} \equiv \frac{1}{2\pi}\int_0^{2\pi} d\theta\, \tilde{\chi}(\psi, \theta).$$

The value of $\tilde{\chi}$ at the origin, $\tilde{\chi}^0$ in Eq. (16), is obtained by fitting the three constants in Eq. (16) to the values of $\langle\chi\rangle$ on the second, third, and fourth magnetic surfaces. Thus, the value of χ at the origin is given as

$$\tilde{\chi}^0 = a_1\overline{\tilde{\chi}(\psi_2)} + a_2\overline{\tilde{\chi}(\psi_3)} + a_3\overline{\tilde{\chi}(\psi_4)}. \tag{17a}$$

where

$$a_1 = (18^{n+1} - 12^{n+1})/d, \tag{17b}$$

$$a_2 = (3^{n+1} - 9^{n+1})/d, \tag{17c}$$

$$a_3 = (4^{n+1} - 2^{n+1})/d, \tag{17d}$$

and

$$d = (18^{n+1} - 12^{n+1}) + (4^{n+1} - 9^{n+1}) + (3^{n+1} - 2^{n+1}). \tag{17e}$$

Step C

The coordinate functions $x_{i,j}$ and $z_{i,j}$ are redefined to be consistent with $\tilde{\chi}^{(k+1)}(\theta, \psi)$. This is done in four parts:

(1) Points are moved along θ_i surfaces so that ψ_j surfaces lie on constant $\bar{\tilde{\chi}}^{(k+1)}$ surfaces (Fig. 2). This is accomplished by first calculating the finite difference form of $\bar{\tilde{\chi}}(\psi_j)$; i.e., for each ψ_j surface we calculate

$$\overline{\tilde{\chi}^{(k+1)}(\psi_j)} = \frac{1}{M} \sum_{i=1}^{M} \tilde{\chi}_{i,j}^{(k+1)}.$$

The coordinates $x_{i,j}^{(k+1/3)}$ and $z_{i,j}^{(k+1/3)}$ are then defined to be the x and z coordinates of the point along the surface θ_i, where $\tilde{\chi}^{(k+1)}(\theta_i, \psi)$ is equal to $\bar{\tilde{\chi}}^{(k+1)}(\psi_j)$. Quadratic interpolation is used to define $\tilde{\chi}^{(k+1)}(\theta_i, \psi)$ between grid points using the arc length along the θ_i surface as the independent variable.

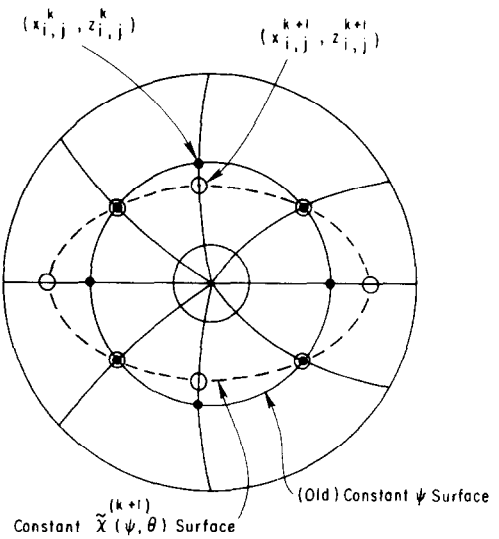

FIG. 2. Points are moved along θ surfaces to lie on constant $\tilde{\chi}^{(k+1)}$ surfaces.

(2) Constant ψ surfaces are respaced to satisfy the surface averaged metric condition. From Eq. (3b), ψ and θ should have the property that

$$d\psi\, d\theta\, \mathscr{J}^{(k+1/3)} = d\psi\, d\theta \left[\mu \left(\frac{x^{(k+1/3)}}{x_0} \right)^m \psi^n \right]. \tag{18}$$

By putting all the θ dependence on the left side of the above equation, integrating from $\theta = 0$ to $\theta = 2\pi$, and then integrating from $\psi = 0$ to $\psi = \psi_j$, we obtain a new value of the coordinate function ψ_j associated with each constant j surface; i.e.,

$$\psi_j = \left[\left(\frac{n+1}{\mu} \right) x_0^m \sum_{j'=1}^{j} \delta\psi \sum_{i=1}^{M} \frac{\delta\theta}{2\pi} \frac{\mathscr{J}_{i,j'}^{(k+1/3)}}{[x_{i,j'}^{(k+1/3)}]^m} \right]^{1/(n+1)}. \tag{19}$$

We define new ψ values linear in j; i.e.,

$$\psi_j^a = \frac{(j-1)}{(N-1)} \psi_N. \tag{20}$$

The coordinates $x_{i,j}^{(k+2/3)}$ and $z_{i,j}^{(k+2/3)}$ are then redefined to be the x and z coordinates of the point along the surface θ_i where $\psi = \psi_j^a$. Quadratic interpolation is again used to define ψ between integral j values. Notice that the constant $[x_0^m(n+1)/\mu]^{[1/(n+1)]}$ is never used in this part of Step C since both ψ_j^a and ψ_j are linear in this term.

(3) Constant θ surfaces are next respaced to satisfy the metric condition within each flux surface. Using Eq. (18) we find that the new value of the coordinate function θ_i associated with each constant i surface is

$$\theta_i = 2\pi \frac{\sum_{i'=1}^{i} \delta\theta\, \mathscr{J}_{i',j}^{(k+2/3)} / [x_{i',j}^{(k+2/3)}]^m}{\sum_{i'=1}^{M} \delta\theta\, \mathscr{J}_{i',j}^{(k+2/3)} / [x_{i',j}^{(k+2/3)}]^m}. \tag{21}$$

For each surface ψ_j we define new θ values linear in i; i.e.,

$$\theta_i^a \equiv \frac{(i-1)}{(M-1)} 2\pi. \tag{22}$$

The coordinates $x_{i,j}^{(k+1)}$ and $z_{i,j}^{(k+1)}$ are finally redefined to be the x and z coordinates of the point along the surface ψ_j where $\theta = \theta_i^a$. The effects of respacing the θ surfaces can be seen in Fig. 3.

(4) Finally, the normalization constant μ is recalculated so that $\psi_N = 1$. From Eq. (19),

$$\psi_N^{n+1} = 1 = \frac{(n+1)}{\mu} x_0^m \sum_{j=1}^{N} \delta\psi \sum_{i=1}^{M} \frac{\delta\theta}{2\pi} \mathscr{J}_{i,j}^{(k+1)} / [x_{i,j}^{(k+1)}]^m. \tag{23}$$

Solving Eq. (23) for μ we obtain

$$\mu = (n+1) x_0^m \sum_{j=1}^{N} \delta\psi \sum_{i=1}^{M} \frac{\delta\theta}{2\pi} \mathscr{J}_{i,j}^{(k+1)} / [x_{i,j}^{(k+1)}]^m. \tag{24}$$

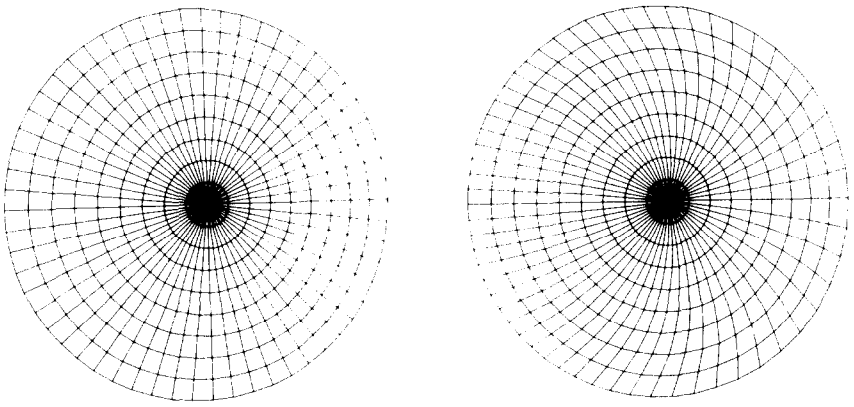

FIG. 3. Before (left) and after (right) respacing the θ lines to satisfy the metric condition on each flux surface.

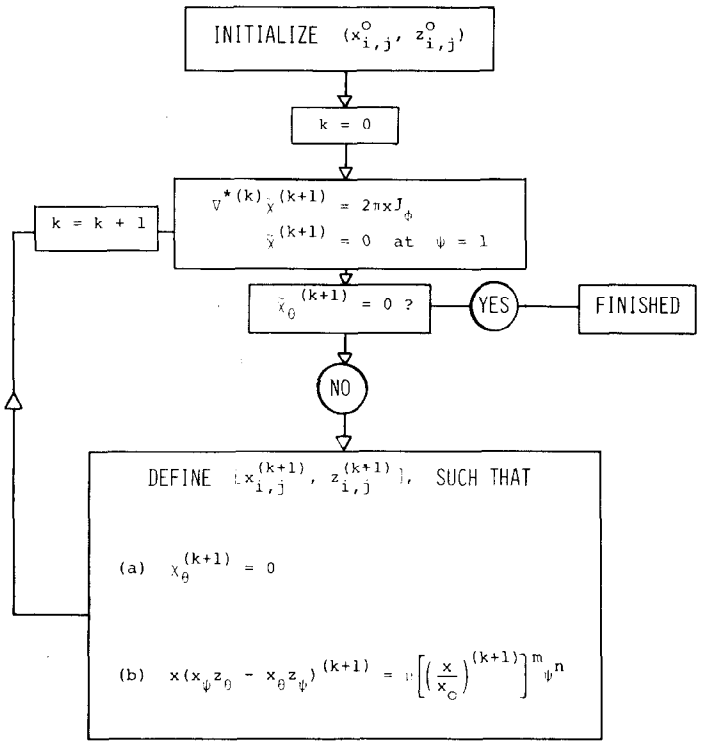

FIG. 4. Flow chart of the solution to the fixed boundary problem.

TABLE I

Number of SOR Iterations Required for Each Metric Iteration for a Typical Fixed Boundary Equilibrium Calculation

k	SOR iterations
0	612
1	315
2	225
3	115
4	53
5	5
6	1

For $m = 1$ and $n = 0$ parts (2) and (3) of this step are equivalent to equalizing the area of each computational zone. A schematic diagram of the solution to the fixed boundary problem is given in Fig. 4.

Each metric iteration through Steps B and C requires successively fewer SOR iterations to converge since the initial conditions for the SOR iteration improve with each successive metric iteration. We show in Table I the number of SOR iterations required for each metric iteration for a typical fixed boundary equilibrium calculation. This had 61 θ zones, 15 w zones, $n = 0$, $m = 1$, with a circular boundary with

and $\varepsilon = 10^{-7}$. It is observed that the number of SOR iterations decreases by approximately a factor of 2 for each successive metric iteration.

Once the equilibrium inside of the plasma has been solved, the vacuum solution can be determined. This is discussed in the next section as part of the free boundary equilibrium problem. A least-squares method for determining a vacuum solution consistent with a plasma of arbitrary shape is discussed in Appendix A.

IV. Free Boundary Solution Method

In the free boundary problem the locations and strengths of K external coils are specified as $\{\mathbf{x}_k;\ k = 1,..., K\}$, $\{I_k;\ k = 1,..., K\}$. The shape of the plasma/vacuum boundary consistent with these current sources is then obtained as part of the solution.

In the plasma region the poloidal flux function χ satisfies

$$x\nabla \cdot (x^{-2}\nabla\chi) = 8\pi^2 x\nabla\phi \cdot \mathbf{J} \tag{25a}$$

and in the vacuum region

$$x\nabla \cdot (x^{-2}\nabla\chi) = 8\pi^2 \sum_{k=1}^{K} I_k \delta(\mathbf{x} - \mathbf{x}_k). \tag{25b}$$

We introduce the free space toroidal Green's function

$$G(\mathbf{x}, \mathbf{x}') = -(xx')^{1/2}[(2-k^2)\,K(k^2) - 2E(k^2)]/k, \tag{26a}$$

where $K(k^2)$ and $E(k^2)$ are complete elliptic integrals and

$$k^2 = 4xx'/[(x+x')^2 + (z-z')^2]. \tag{26b}$$

This satisfies

$$x\nabla \cdot [x^{-2}\nabla G(\mathbf{x}, \mathbf{x}')] = 2\pi\delta(\mathbf{x} - \mathbf{x}'). \tag{27}$$

Green's theorem can be used to express the solution of Eq. (25) in the form

$$\chi(\mathbf{x}_T) = 4\pi \int dA\; x\nabla\phi \cdot \mathbf{J} G(\mathbf{x}_T, \mathbf{x}) + \sum_{k=1}^{K} 4\pi I_k G(\mathbf{x}_T, \mathbf{x}_k), \tag{28}$$

where the surface integral is over the plasma cross section. The free constant in the solution for χ has been chosen so that χ vanishes far from the plasma.

The surface integral appearing in Eq. (28) is expensive to evaluate numerically. It can be converted to a line integral by noting that if $\tilde{\chi}$ satisfies

$$x\nabla \cdot (x^{-2}\nabla\tilde{\chi}) = 8\pi^2\, x\nabla\phi \cdot \mathbf{J} \tag{29}$$

in the plasma region and vanishes on the plasma boundary, then Green's theorem can again be used to express Eq. (28) in the form

$$\chi(\mathbf{x}_T) = \oint \frac{dl}{2\pi x} G(\mathbf{x}_T, \mathbf{x}) \frac{\partial\tilde{\chi}}{\partial n} + \sum_{k=1}^{K} 4\pi I_k G(\mathbf{x}_T, \mathbf{x}_k) \tag{30a}$$

if the point $\mathbf{x}_T$ is outside the plasma, and

$$\chi(\mathbf{x}_T) = \oint \frac{dl}{2\pi x} G(\mathbf{x}_T, \mathbf{x}) \frac{\partial\tilde{\chi}}{\partial n} + \sum_{k=1}^{K} 4\pi I_k G(\mathbf{x}_T, \mathbf{x}_k) + \tilde{\chi}(\mathbf{x}_T) \tag{30b}$$

if the point $\mathbf{x}_T$ is inside the plasma.

The contour of integration is the plasma/vacuum interface. Equation (30) is easily extended to include an outer wall of finite radius. This is discussed in Appendix B.

The solution of the free boundary problem consists of the following steps:

A. Give the positions and strenghts of K external conductors and the locations of p limiter points.

B. Guess an initial shape for the plasma/vacuum boundary corresponding to outer iteration level $q = 0$:

$$[x_{i,N}^{(q)}, z_{i,N}^{(q)}], \qquad i = 1,..., M.$$

C. Determine $\tilde{\chi}^{(q)}(\psi)$ inside the level q set of boundary points by the procedure described in Section III.

D. Using Eq. (30) to define $\chi^{(q+1)}$ as a functional of $\tilde{\chi}^{(q)}$ and the external conductors, define χ_{lim} to be the minimum value of $\chi^{(q+1)}$ among all the limiter points.

E. Define the boundary points $[x_{i,N}^{(q+1)}, z_{i,N}^{(q+1)}]$ as the points along the constant θ_i contours where $\chi^{(q+1)}$ from Eq. (30) is equal to χ_{lim} from Step D (see Fig. 5).

F. Iterate Steps C through E until the new boundary points in E are the same as the old boundary points to some tolerance.

To locate the new boundary points in Step E, a binary search for χ_{lim} is carried out along lines which are straight outside of the plasma/vacuum boundary and are constant θ lines inside. Equation (30) is used to define χ everywhere. The line integral is approximated by M line segments Δl_s. For example, for $\mathbf{x}_T$ inside the plasma/vacuum interface we have

$$\chi^{(q+1)}(\mathbf{x}_T) = \tilde{\chi}^{(q)}(\mathbf{x}_T) + \sum_{i=1}^{M} \frac{\Delta l_i}{2\pi x_{i,N}} G(\mathbf{x}_T, \mathbf{x}_{i,N}) \left(\frac{\partial \tilde{\chi}^{(q)}}{\partial n}\right)_i + \sum_{k=1}^{K} 4\pi I_k G(\mathbf{x}_T, \mathbf{x}_k). \tag{31a}$$

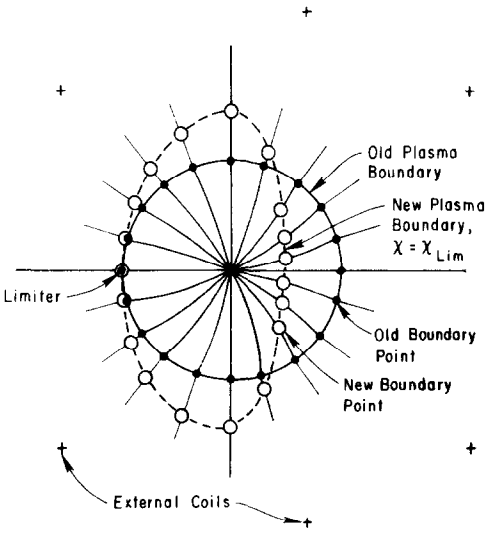

FIG. 5. Redefine the plasma/vacuum boundary as the $\chi = \chi_{\text{lim}}$ surface.

Special care must be taken for $\mathbf{x}_T$ lying on the plasma/vacuum boundary since $|G(\mathbf{x}_T, \mathbf{x}_s)|$ becomes singular as $\mathbf{x}_T$ approaches $\mathbf{x}_s$. Thus, for $\mathbf{x}_T$ coinciding with one of the boundary points $\mathbf{x}_{T,N}$, we have

$$\chi^{(q+1)}(\mathbf{x}_T) = \sum_{\substack{i=1 \\ i \neq T}}^{M} \frac{\Delta l_i}{2\pi x_{i,N}} G(\mathbf{x}_T, \mathbf{x}_{i,N}) \left(\frac{\partial \tilde{\chi}^{(q)}}{\partial n}\right)_i$$

$$+ \int_{\Delta l_T} \frac{dl}{2\pi x} G(\mathbf{x}_T, \mathbf{x}) \left(\frac{\partial \tilde{\chi}^{(q)}}{\partial n}\right) + \sum_{k=1}^{K} 4\pi I_k G(\mathbf{x}_T, \mathbf{x}_k), \tag{31b}$$

where the "self field" term can be approximated by

$$\int_{\Delta l_T} \frac{dl}{2\pi x} G(\mathbf{x}_T, \mathbf{x}) \left(\frac{\partial \tilde{\chi}^{(q)}}{\partial n}\right) \simeq \left(\frac{\partial \tilde{\chi}^{(q)}}{\partial n}\right)_T \frac{\Delta l_T}{2\pi} \left[\ln\left(\frac{\Delta l_T}{16 x_{T,N}}\right) + 1\right]. \tag{31c}$$

The terms $(\partial\tilde{\chi}/\partial n)$ in Eq. (31) are approximated by a second order accurate finite difference formula applied at the plasma boundary $j = N$

$$\left(\frac{\partial \tilde{\chi}^{(q)}}{\partial n}\right)_i = |\nabla\psi|_{i,N} (-4\tilde{\chi}^{(q)}_{i,N-1} + \tilde{\chi}^{(q)}_{i,N-2})/(2\delta\psi). \tag{32}$$

V. Verification and Applications

We can test the accuracy of the iterative metric method by numerically calculating the solution to a problem for which the analytic solution is known [9]. The solution to the equilibrium equation for p' equal to a constant and gg' equal to zero, i.e., $\alpha = 1$ in Eq. (3) and $\beta \equiv 0$ in Eq. (4), can be written

$$\chi(x, z) = \chi(1) + [\chi(0) - \chi(1)] f(x, z), \tag{33a}$$

where

$$f(x, z) \equiv 1 - (SR)^{-2} [x^2 z^2 + (\eta/4)(x^2 - R^2)^2] \tag{33b}$$

and

$$\eta \equiv 8\pi^3 p_0 \left(\frac{RS}{\chi(1) - \chi(0)}\right)^2 - 1. \tag{33c}$$

R is the distance from the symmetry axis to the magnetic axis, S is the perpendicular distance from the magnetic axis to the plasma vacuum boundary, p_0 is the pressure at the magnetic axis, $\chi(0)$ and $\chi(1)$ are the poloidal fluxes at the magnetic axis and the plasma/vacuum boundary respectively, $(1 - \eta^{-1})^{1/2}$ is the ellipticity at the magnetic axis for $\eta \geqslant 1$ and $\pi S^2 x_0 / R[\chi(1) - \chi(0)]$ is the safety factor at the magnetic axis for $\eta = 1$. The plasma/vacuum boundary is given by the equation $f(x, z) = 0$. Using the

procedure described in Section III, we solve the equilibrium equation inside the boundary using a very fine tolerance for the SOR iteration. Letting $\bar{\chi}_{ij}$ equal the poloidal flux at $(x_{i,j}, z_{i,j})$ given by Eq. (33), and x_{axis} equal the position of the magnetic axis given by the numerical solution we calculate the quantities

$$\chi_{\text{err}} \equiv [MN|\chi(1)-\chi(0)|]^{-1} \sum_{j=1}^{N} \sum_{i=1}^{M} |\tilde{\chi}_{i,j} - [\bar{\chi}_{i,j} - \chi(1)]| \tag{34a}$$

and

$$x_{\text{err}} \equiv R^{-1}|R - x_{\text{axis}}| \tag{34b}$$

for several combinations of M and N. Values of χ_{err} and x_{err} for $S=1$, $R=5$, $\chi(1)=0$, $\chi(0)=-1.759$, $\eta=1$, and several combinations of M and N are given in Tables IIa and IIb. The values of χ_{err} and x_{err} are seen to decrease as the number of both ψ and θ zones increase.

To test the free boundary method, we first generate a set of coil currents which gives a vacuum solution to the fixed boundary test just described. This is accom-

TABLE IIa

χ_{err} in Units of 10^{-4} (Eq. (34a))

M	N		
	10	15	20
20	6.57	7.93	8.56
40	4.57	1.96	1.54
60	4.98	1.96	1.02

TABLE IIb

x_{err} in Units of 10^{-4} (Eq. (34b))

M	N		
	10	15	20
20	7.90	2.96	1.11
40	9.03	4.08	2.26
60	9.18	4.29	2.46

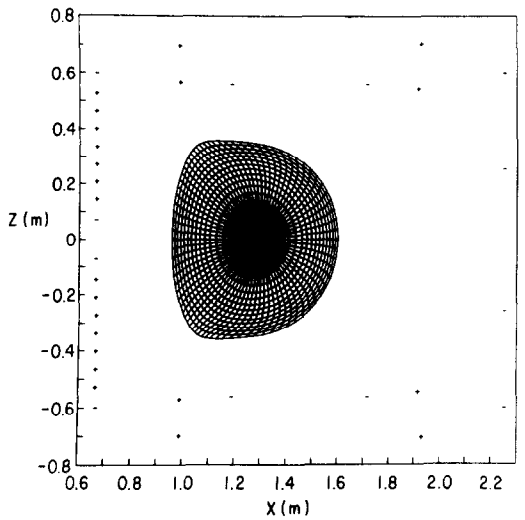

FIG. 6. Flux surfaces of a standard Princeton Poloidal Divertor Experiment equilibrium.

plished using the least-squares method described in Appendix A. We then look for the solution to the equilibrium equation using the p and g procedure described in Section IV with the input $\alpha = 1$ and I_T equal to the toroidal current from the fixed boundary test. The quantity γ is constrained to be zero for this test and the limiter is one point $(x_{\text{lim}}, z_{\text{lim}})$ such that $f(x_{\text{lim}}, z_{\text{lim}}) = 0$. The numerical solution with 48 θ zones and 18 ψ zones gives the position of the magnetic axis as 4.996, the poloidal flux at the axis as -1.771, and the safety factor at the axis as 1.603. The position of

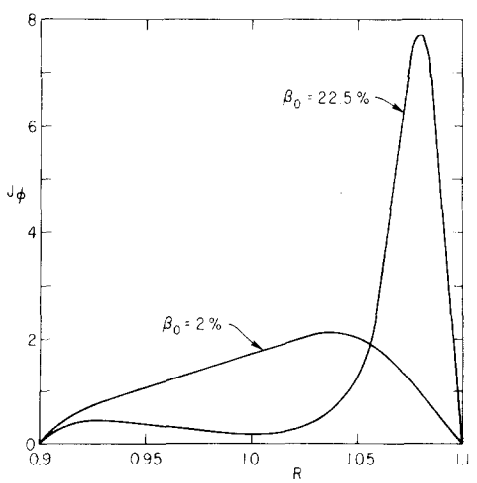

FIG. 7. Midplane current density profiles for various values of β_T.

the magnetic axis, the poloidal flux on axis, and the safety factor at the axis given by the analytic solution are respectively 5.000, −1.759, and 1.614.

One of the applications of the iterative metric method is to generate Princeton Poloidal Divertor Experiment (PDX) equilibria for subsequent axisymmetric stability analysis. The limiting value of the poloidal flux in a PDX plasma is chosen to be slightly less than the flux at the separatrix in the poloidal magnetic field. In Fig. 6 the flux surfaces of a typical PDX plasma are shown. The total plasma current is 500 kA. Other parameters are $\alpha = \beta = 2$, $m = 1$, $n = 0$, $M = 40$, $N = 15$, and $x_0 = 1.25$. The magnetic axis for this case lies at $x = 128.41$ cm.

An instance in which this equilibrium solution method proved invaluable was in

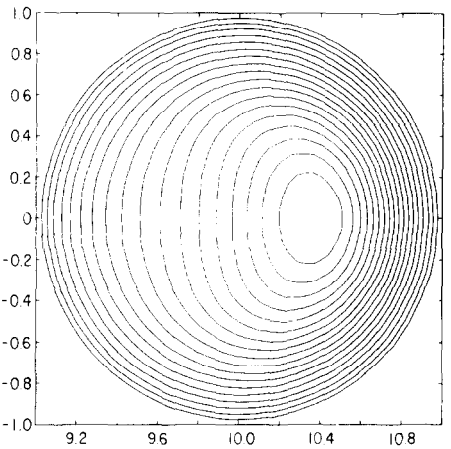

FIG. 8a. Current contours for $\beta_T = 0.020$.

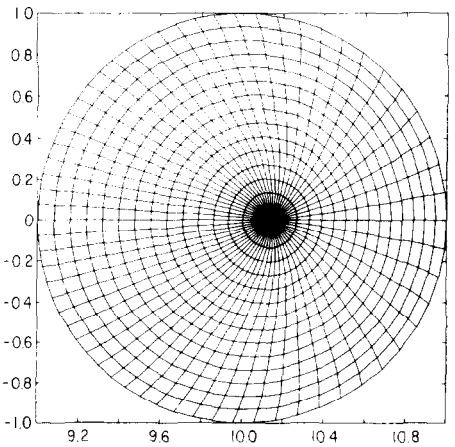

FIG. 8b. Flux surfaces for $\beta_T = 0.020$.

the study of high beta internal mode stability [8]. Initial attempts to generate equilibria for stability analysis using the functional forms of Eqs. (11e) and (11f) in the standard (x, ϕ, z) equilibrium code [2], were unsuccessful at values of $\beta_T \equiv 8\pi p/B_T^2 \gtrsim a/R$. Consideration of the midplane current density profiles for various values of β_T as shown in Fig. 7 illustrates the problem. For $\beta_T \gtrsim R/a \sim 0.1$, the current density is small throughout most of the plasma with a large spike at the outer plasma edge. Resolution of the current density in real space is poor because of the spatially localized gradients. However, in flux space, the grid is naturally crowded towards the region of large gradients and accurate solutions are obtainable. Sequences of equilibria with fixed $q(\chi)$, $\Delta\chi$ and varying p_0 were generated from $\beta_T = 0$ to $\beta_T = 0.25$. Figures 8 and 9 show solutions at $\beta_T = 0.020$ and $\beta_T = 0.225$. Both

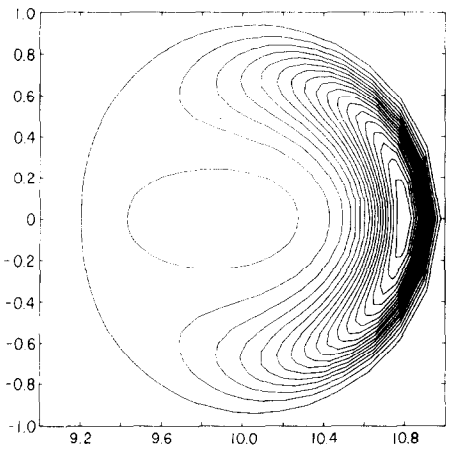

FIG. 9a. Current contours for $\beta_T = 0.225$.

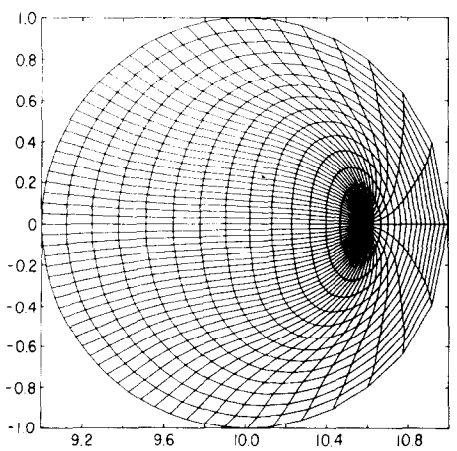

FIG. 9b. Flux surfaces for $\beta_T = 0.225$.

have $\alpha = 4$, $\beta = 1$, and $\Delta\chi = 0.375$. These equilibria were used to analyze the ideal internal and free surface mode stability [3] as a function of β_T. These results confirmed the existence of a high β region of stability to internal modes, and demonstrated high β saturation of the free surface modes.

VI. Summary and Discussion

A new algorithm has been described for the calculation of MHD equilibria of axisymmetric toroidal plasmas. The method uses finite differences in a generalized coordinate system which is iterated for simultaneously with the equilibrium solution until one coordinate coincides with the magnetic surfaces. Special treatment of the difference equations to yield accurate solutions near the magnetic axis is discussed.

The method described here automatically accumulates grid points in regions of steep gradients, thus yielding accurate solutions of high β equilibria. The pressure $p(\chi)$ and either the toroidal field function $g(\chi)$ or the safety factor $q(\chi)$ can be prescribed, allowing computation of sequences of FCT equilibria where $q(\chi)$ remains fixed. Solution procedures for both fixed boundary equilibria where the shape of the outer magnetic flux surface is prescribed, and free boundary equilibria where a set of external coils define the magnetic boundary conditions have been described, and examples of each are given. Comparison of computed solutions with an analytic equilibrium illustrate accuracy and convergence properties.

The advantages of obtaining equilibrium using magnetic field line coordinates have been recognized for some time. Potter [10] describes a pseudotime advancement algorithm based on the water bag method for allowing residual forces to push magnetic surfaces to equilibrium. While successful, this method suffers an intrinsic inefficiency resulting from the wide range of time scales physically present in the normal modes of the plasma. Low-frequency motions with small restoring forces take a large number of computational cycles to relax to equilibrium.

More recently, a finite element method for obtaining MHD equilibrium solutions has been described by Takeda *et al.* [11]. In this work, as with the present method, the mesh structure is iteratively solved for together with the poloidal flux solution, so that the final solution has finite elements aligned along magnetic surfaces. However, it does not allow for the specification of the rotational transform $q(\chi)$ and it does not solve free boundary problems in which the external coils determine the shape of the outer magnetic flux surface.

Appendix A

We can obtain a vacuum solution [2] consistent with a plasma of arbitrary shape by calculating a set of coil currents which minimize the least-squares error between the desired value of flux on the boundary and the value given by Eq. (30a). If

we let $\mathbf{x}_{bj}$ denote the jth boundary point and $\mathbf{x}_k$ the position of the kth coil, we can obtain a linear system for the currents by minimizing the quantity

$$\varepsilon = \sum_{j=1}^{M} \left(\chi_1 - \oint \frac{dl}{2\pi x} G(\mathbf{x}_{bj}, \mathbf{x}) \frac{\partial \tilde{\chi}}{\partial n} - \sum_{k=1}^{K} 4\pi I_k G(\mathbf{x}_{bj}, \mathbf{x}_k) \right)^2 + \Gamma \sum_{k=1}^{k} 4\pi I_k^2, \tag{35}$$

where χ_1 is the desired value of poloidal flux on the plasma/vacuum boundary and Γ is a (small) quantity which may be needed for numerical stability. Thus,

$$\frac{1}{2} \frac{\partial \varepsilon}{\partial I_l} = \sum_{j=1}^{M} \left(-\chi_1 + \oint \frac{dl}{2\pi x} G(\mathbf{x}_{bj}, \mathbf{x}) \frac{\partial \tilde{\chi}}{\partial n} + \sum_{k=1}^{K} 4\pi I_k G(\mathbf{x}_{bj}, \mathbf{x}_k) \right) \times G(\mathbf{x}_{bj}, \mathbf{x}_l) + \Gamma I_l = 0 \tag{36a}$$

or

$$\mathbf{A} \cdot \mathbf{B} = \mathbf{C}, \tag{36b}$$

where

$$A_{lm} = \sum_{j=1}^{M} G(\mathbf{x}_{bj}, \mathbf{x}_l)\, G(\mathbf{x}_{bj}, \mathbf{x}_m) + \Gamma \delta_{lm}, \tag{36c}$$

$$B_m = 4\pi I_m, \tag{36d}$$

$$C_l = \sum_{j=1}^{M} \left(\chi_1 - \oint \frac{dl}{2\pi x} G(\mathbf{x}_{bj}, \mathbf{x}) \frac{\partial \tilde{\chi}}{\partial n} \right) G(\mathbf{x}_{bj}, \mathbf{x}_l). \tag{36e}$$

Equation (36) is solved numerically for the I_m using standard LU decomposition.

Appendix B

Here we consider the vacuum solution when a conducting wall of arbitrary shape surrounds the vacuum region. The analog of Eq. (30) now reads

$$\chi(\mathbf{x}_T) - \chi_w = \oint_p \frac{dl}{2\pi x} G(\mathbf{x}_T, \mathbf{x}) \frac{\partial \tilde{\chi}}{\partial n} + \sum_{k=1}^{K} 4\pi I_k G(\mathbf{x}_T, \mathbf{x}_k) - \oint_w \frac{dl}{2\pi x} G(\mathbf{x}_T, \mathbf{x}) \frac{\partial \chi}{\partial n} \tag{37a}$$

if the point $\mathbf{x}_T$ is in the vacuum region, and

$$\chi(\mathbf{x}_T) - \chi_w = \oint_p \frac{dl}{2\pi x} G(\mathbf{x}_T, \mathbf{x}) \frac{\partial \tilde{\chi}}{\partial n} + \sum_{k=1}^{K} 4\pi I_k G(\mathbf{x}_T, \mathbf{x}_k) - \oint_w \frac{dl}{2\pi x} G(\mathbf{x}_T, \mathbf{x}) \frac{\partial \chi}{\partial n} + \tilde{\chi}(\mathbf{x}_T) \tag{37b}$$

if $\mathbf{x}_T$ is the plasma region. Here, χ_w is the poloidal flux at the wall and the two line integrals are over the plasma/vacuum interface and the wall.

If Eq. (37) is to be used to define $\chi(\mathbf{x}_T)$, $\partial\chi/\partial n$ must be known at the wall. To obtain this, Eq. (37a) is evaluated at J points $(\mathbf{x}_{bj}, j = 1,..., J)$ equally spaced around the outer wall. Thus, we obtain the linear system

$$a_{ij}\left(\frac{\partial\chi}{\partial n}\right)_j = b_i, \tag{38a}$$

where

$$b_i = \oint \frac{dl}{2\pi x} G(\mathbf{x}_{bi}, \mathbf{x}) \frac{\partial\tilde{\chi}}{\partial n} + \sum_{k=1}^{K} 4\pi I_k G(\mathbf{x}_{bi}, \mathbf{x}_k), \tag{38b}$$

$$a_{ij} = \frac{\Delta l_j}{2\pi x_{bj}} G(\mathbf{x}_{bi}, \mathbf{x}_{bj}) \qquad \text{for} \quad i \neq j, \tag{38c}$$

$$a_{ii} = \frac{\Delta l_i}{2\pi}\left[ln\left(\frac{\Delta l_i}{16 x_{bi}}\right) + 1\right]. \tag{38d}$$

The system Eq. (38a) is inverted to give $\partial\chi/\partial n$ at the wall. This is then used to evaluate the wall integral in Eq. (37) and one proceeds as with Eq. (30).

ACKNOWLEDGMENTS

It is a pleasure to acknowledge useful discussions with J. L. Johnson, J. M. Greene, M. Okabayashi, and S. Dalhed. The authors are grateful to one of the reviewers for making them aware of the existence of Ref. [11].

This work was supported by the United States Department of Energy under Contract EY-76-C-02-3073.

REFERENCES

1. H. GRAD, O. N. HU, AND D. C. STEVENS, *Proc. Nat. Acad. Sci. USA* **72** (1975), 3789.
2. J. L. JOHNSON, H. E. DALHED, J. M. GREENE, R. C. GRIMM, Y. Y. HSIEH, S. C. JARDIN, J. MANICKAM, M. OKABAYASHI, R. G. STORER, A. M. M. TODD, D. E. VOSS, AND K. E. WEIMER, *J. Comput. Phys.* **32** (1979), 212.
3. J. S. CALLEN AND R. A. DORY, *Phys. Fluids* **15** (1972), 1532.
4. F. J. HELTON AND T. S. WANG, *Nucl. Fusion* **18** (1978), 11.
5. R. C. GRIMM, J. M. GREENE, AND J. L. JOHNSON, *Methods Comput. Phys.* **16** (1976), 253.
6. S. C. JARDIN, J. L. JOHNSON, J. M. GREENE, AND R. C. GRIMM, *J. Comput. Phys.* **29** (1978), 101.
7. S. P. HIRSHMAN AND S. C. JARDIN, *Phys. Fluids* **22** (1979), 731.
8. H. R. STRAUSS, W. PARK, D. A. MONTICELLO, R. B. WHITE, S. C. JARDIN, M. S. CHANCE, A. M. M. TODD, AND A. H. GLASSER, *Phys. Rev. Lett.*, in press.
9. M. S. CHANCE, J. M. GREENE, R. C. GRIMM, J. L. JOHNSON, J. MANICKAM, W. KERNER, D. BERGER, L. C. BERNARD, R. GRUBER, AND F. TROYON, *J. Comput. Phys.* **28** (1978), 1.
10. D. POTTER, *Methods Comput. Phys.* **16** (1976), 43.
11. T. TAKEDA AND T. TSUNEMATSU, JAERI-M 8042, Japan Atomic Energy Research Institute, 1979.